Springer

Journal of Mechanical Science and Technology 23 (2009) 1553~1562

Journal of Mechanical Science and Technology

www.springerlink.com/content/1738-494x
DOI 10.1007/s12206-009-0423-3

Finite volume method analysis of heat transfer problem using adapted strongly implicit procedure †

Abel Rouboa[1,*], Eliseu Monteiro[2] and Regina de Almeida[3]

[1]*CITAB-UTAD/Department of Mechanical Engineering and Applied Mechanics, University of Pennsylvania, PA-19104-639*
[2]*Engineering Department, University of Trás-os-Montes e Alto Douro, P-5000-911 Vila Real, Portugal*
[3]*Mathematical Department, University of Trás-os-Montes e Alto Douro, P-5000-911 Vila Real, Potugal*

(Manuscript Received June 9, 2008; Revised December 31, 2008; Accepted March 11, 2009)

Abstract

In most issues representing physical problems, the complex geometry cannot be represented by a Cartesian grid. The multi-block grid technique allows artificially reducing the complexity of the geometry by breaking down the real domain into a number of sub-domains with simpler geometry. The main aim of this article is to show the usefulness of simple solvers in complex geometry problems, when using curvilinear coordinates combined with multi-block grids. This requires adapted solvers to a nine nodes computational cell instead of the five nodes computational cell used with Cartesian coordinates for two-dimensional cases. These developments are presented for the simple iterative methods Jacobi and Gauss-Seidel and also for the incomplete factorization method strongly implicit procedure (SIP). These adapted solvers are tested in two cases: a simple geometry (heat transfer in a circular cross-section) and a complex geometry (solidification case). Results of the simple geometry case show that all the adapted solvers have good performance with a slight advantage for the SIP solver. For increasing the complexity of the geometry, the results showed that Jacobi and Gauss-Seidel solvers are not suitable. However, the SIP method has a reasonable performance. A conclusion could be drawn that the SIP method could be used in complex geometry problems using multi-block grid technique when high precision results are not required.

Keywords: Curvilinear coordinates; Heat transfer; Multi-block grid; Strongly implicit procedure

1. Introduction

In most issues representing physical problems, the geometry cannot be represented by a Cartesian grid; instead, it is common for the boundaries to be curved in space. A structured mesh is topologically rectangular which can be deformed in space such that it is no longer Cartesian but may still be orthogonal. Such a mesh can be difficult to generate, and so a completely general grid will be non-orthogonal with no restriction on the angles of the grid lines intersections.

With the development of computer hardware, numerical simulation has made rapid progress. Most commercial software packages have become more and more practical but not efficient in terms of their adaptation to complex geometry and/or inadequate boundary conditions.

For complex geometry problems adequate numerical methods using unstructured mesh are known. For an overview on unstructured mesh techniques see for example [1].

In the last few decades intensive studies have been done to model various problems, for example: to solve radiative transfer problem in triangular meshes [2] using discrete transfer method (DTM [3]), Galerkin finite element method used to study the turbulent fluid flow and heat transfer problems in a domain with moving phase-change boundary [4, 5] and also to

† This paper was recommended for publication in revised form by Associate Editor Jun Sang Park
*Corresponding author. Tel.: +0012158987998, Fax.: +0012155736334
E-mail address: rouboa@seas.upenn.edu

solve nonlinear phenomena [6].

Finite volume (FV) method for the calculation of solute transport in directional solidification has been studied and validated in [7]. Finite element (FE) method to model the filling and solidification inside a permanent mold is performed in [8]. Three-dimensional parallel simulation tool using an unstructured FV method with Jacobian-free Newton-Krylov solver has been done in [9] for solidifying flow applications. Also, arbitrary Lagrangian-Euler (ALE) formulation was developed in [10] to simulate casting processes, among others.

The strongly implicit procedure (SIP) is known for solving the system of algebraic equations that arises, for instance, in the finite differences (FD) or finite analytic description of field problems [11]. This procedure was also used in multi-phase fluid flow and heat transfer problems [12].

In the present work the SIP also known as Stone's solver, is adapted to solve a linear equation system from FV discretization of two-dimensional heat transfer problems in simple and complex geometries. From the FV discretization procedure one obtains a linear equation system of the form $A\theta = Q$ where A is a sparse matrix, θ the variable in computation and Q a vector of independent terms. The coefficient matrix will typically take a hepta diagonal structure, with the non-zero components occupying only seven diagonals of the matrix. For two-dimensional partial differential equations (PDE) there will be only five diagonals which are non-zero. For unstructured meshes, the coefficient matrix will also take a diagonal structure, with the non-zero components occupying nine diagonals of the matrix for two-dimensional cases. This regular structure enables a considerable reduction in memory use and the number of operations performed.

In this paper the development of the classical solvers (Jacobi, Gauss-Seidel) and SIP (strongly implicit procedure) is presented in order to be used with curvilinear coordinates systems in two-dimensional domains. The main aim is to apply these methods to non-orthogonal grids. Two examples are given to demonstrate the validity of the method. In the first case a simple geometry (heat transfer in a circular cross-section) is obtaining not only a numerical but also an analytical solution of the thermal evolution of a slab with infinite length and circular cross section. The second case is a classical example of a multi-physics phenomena-casting process. Normally, complex geometry problems are solved using moving boundary techniques, but in this paper we use multi-block grid. We study the possibility of using simple iterated methods (Jacobi and Gauss-Seidel) and an incomplete factorization method SIP instead of using, for example, Krylov space methods.

2. Governing linear system

From the discretization process of the heat transfer phenomena, no matter which method is used, the result is an algebraic equation system. This can, in general (see e.g. [13-15]), be written as the following linear system:

$$A\theta = Q \tag{1}$$

where A is a sparse matrix, θ is a vector which is the computational variable, and Q is a vector of independent terms. The structure of the matrix A depends on the ordering of the variables in the vector θ. As in [13] one orders the entries in the vector θ starting at the southwest corner of the domain, proceeding northwards along each grid and then eastward across the domain.

The algebraic equation for a particular control volume in a two-dimensional domain, see Fig. 1, using curvilinear coordinates, is of the form:

$$A_P\theta_P + \sum_{nb} A_{nb}\theta_{nb} = Q_P \tag{2}$$

where P represents the node where the partial differential equation value is calculated and the index nb represents the neighborhood nodes involved in the approach. Using a geographical notation: E (east), N

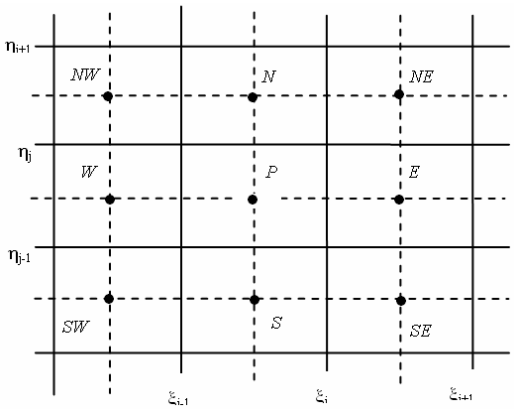

Fig. 1. Typical two-dimensional control volume.

(north), S (south), W (west), NE (northeast), NW (northwest), SE (southeast), SW (southwest), the sum is extended in the following form:

$$\sum_{nb} A_{nb}\theta_{nb} = A_E\theta_E + A_W\theta_W + A_N\theta_N + A_S\theta_S + A_{NE}\theta_{NE} + A_{SE}\theta_{SE} + A_{NW}\theta_{NW} + A_{SW}\theta_{SW} \quad (3)$$

The properties of the linear system Eq. (1) are important when setting up an iteration method for its solutions. Let us present some of the classical iteration methods modified to the problem treated here.

2.1 Jacobi's method

In the Jacobi method, the resulting equations from the discretization process are determined separately. Eq. (3) is modified assuming the following form:

$$\theta_P = A_P^{-1}\left(Q_P - \sum_{nb\neq P} A_{nb}\theta_{nb}\right) \quad (4)$$

Having the following iterative method defined as

$$\theta_P^k = A_P^{-1}\left(Q_P - \sum_{nb\neq P} A_{nb}\theta_{nb}^{(k-1)}\right) \quad (5)$$

where all the terms of the Eq. (5) are related to the last iteration release. In the Jacobi method, the values used are of the previous iteration in a way to get the values of the following iteration. However, when we are calculating the new, the actual value is already known.

2.2 Gauss-Seidel's method

The Gauss-Seidel method, in contrast with the Jacobi method, uses the actual values instead of the ones of the previous iteration (see [14, 16]). This idea leads to the following modification of Eq. (5):

$$\theta_P^k = A_P^{-1}Q_P - A_P^{-1}\sum_{nb\in\{SW,W,NE,S\}} A_{nb}\theta_{nb}^{(k)} - A_P^{-1}\sum_{nb\in\{N,NE,E,SE\}} A_{nb}\theta_{nb}^{(k)} \quad (6)$$

Usually, this method converges faster than the Jacobi method.

2.3 SIP method

The SIP solver is an advanced version of the incomplete LU decomposition [17]:

$$M = LU \quad (7)$$

where M is the iterative matrix, L (lower triangular) and U (upper triangular) matrices. The matrix M is given by the splitting of the matrix A in the form $M = A + N$, such that M is a good approximation to A.

This method will be described for a nine-point computational cell (see Fig. 1). The L (lower) and U (upper) matrices have non-zero elements only on diagonals on which A has non-zero elements. The product of lower and upper triangular matrices with these structures has more non-zero diagonals than A.

For the nine-point computational cell there are four diagonals (corresponding to nodes NN (north-north), NNW (nor-northwest), SS (south-south), SSE (south-southeast), SS (south-south)) as can be seen in Fig. 2.

The nine sets of elements (five in L and four in U) are determined by using the rules of multiplication matrix as follows:

$$\begin{aligned}
M_{SW} &= L_{SW}\\
M_W &= L_{SW}U_N + L_W\\
M_{NW} &= L_W U_N + L_{NW}\\
M_{NNW} &= L_{NW}U_N\\
M_{SS} &= L_{SW}U_{SE}\\
M_S &= L_{SW}U_E + L_W U_{SE} + L_S\\
M_P &= L_{SW}U_{NE} + L_W U_E + L_{NW}U_{SE} + L_S U_N + L_P\\
M_N &= L_W U_{NE} + L_{NW}U_E + L_P U_N\\
M_{NN} &= L_{NW}U_{NE}\\
M_{SSE} &= L_S U_{SE}\\
M_{SE} &= L_S U_E + L_P U_E\\
M_E &= L_S U_{NE} + L_P U_E\\
M_{NE} &= L_P U_{NE},
\end{aligned} \quad (8)$$

We wish to select matrices L and U in order to obtain M as a good approximation to A and consequently have a faster convergence of the method. For this reason the matrix N must contain, at least, the four diagonals of the matrix M which correspond to zero diagonals of A. Furthermore, N has to have non-zero elements only on these diagonals. Therefore, the other diagonals of matrix M have the corresponding diagonals of A.

In [17], Stone recognized that convergence can be improved by allowing matrix N to have non-zero elements on the diagonal corresponding to all thirteen

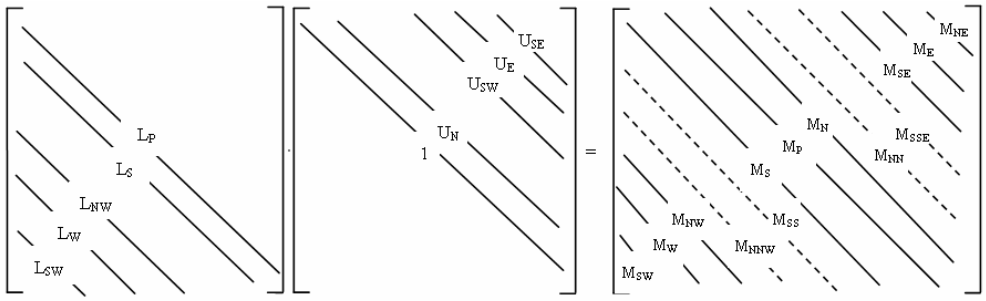

Fig. 2. Schematic presentation of the matrices *L* (Lower), *M* (Upper) and the product matrix *M*;diagonals of *M* not found in *A* are shown by dashed lines.

non-zero diagonals of *LU*. Considering the vector $M\theta$, the method can be easily derived:

$$\begin{aligned}(M\theta)_P &= M_P\theta_P + M_S\theta_S + M_N\theta_N + M_E\theta_E \\ &+ M_W\theta_W + M_{NE}\theta_{NE} + M_{NW}\theta_{NW} \\ &+ M_{SE}\theta_{SE} + M_{SW}\theta_{SW} + M_{NNW}\theta_{NNW} \\ &+ M_{SSE}\theta_{SSE} + M_{NN}\theta_{NN} + M_{SS}\theta_{SS}\end{aligned} \tag{9}$$

Each term in this equation corresponds to a diagonal of $M = LU$. The matrix *N* must contain the four last terms which are the extra diagonals of *M*, and the elements on the remaining diagonals, are chosen so that $N\theta \approx 0$:

$$\begin{aligned}&N_P\theta_P + N_S\theta_S + N_N\theta_N + N_E\theta_E + \\ &+N_W\theta_W + N_{NE}\theta_{NE} + N_{NW}\theta_{NW} + \\ &+N_{SE}\theta_{SE} + N_{SW}\theta_{SW} + N_{NNW}\theta_{NNW} + \\ &+N_{SSE}\theta_{SSE} + N_{NN}\theta_{NN} + N_{SS}\theta_{SS} \approx 0\end{aligned} \tag{10}$$

This requires that the contribution of the four extra terms, in the above equation, have to be nearly cancelled by the contribution of other diagonals, i.e., Eq. (9) should be reduced to the following expression:

$$\begin{aligned}&M_{NNW}\left(\theta_{NNW} - \theta^*_{NNW}\right) + M_{SSE}\left(\theta_{SSE} - \theta^*_{SSE}\right) \\ &+M_{NN}\left(\theta_{NN} - \theta^*_{NN}\right) + M_{SS}\left(\theta_{SS} - \theta^*_{SS}\right) \approx 0,\end{aligned} \tag{11}$$

where $\theta^*_{NNW}, \theta^*_{SSE}, \theta^*_{NN}, \theta^*_{SS}$ are approximations of $\theta_{NNW}, \theta_{SSE}, \theta_{NN}, \theta_{SS}$, respectively.
The proposed approximation in this study is:

$$\begin{aligned}\theta^*_{NNW} &= \alpha\left(\theta_{NW} + \theta_N + \theta_W - 2\theta_P\right) \\ \theta^*_{NN} &= \alpha\left(\theta_N + \theta_{NE} + \theta_{NW} - 2\theta_P\right) \\ \theta^*_{SS} &= \alpha\left(\theta_S + \theta_{SW} + \theta_{SE} - 2\theta_P\right) \\ \theta^*_{SSE} &= \alpha\left(\theta_S + \theta_{SE} + \theta_E - 2\theta_P\right),\end{aligned} \tag{12}$$

where $\alpha < 1$ by stability reasons.
Substituting (12) into Eq. (11) and comparing the result with Eq. (10), we obtain all elements of matrix *N* as linear combinations of M_{NNW} M_{SSE}, M_{NN} and M_{SS}. Elements of the matrix *M* can be set equal to the sum of matrix elements of *A* and *N*.

The resulting equations are not only sufficient to determine all of the elements of the matrix *L* and *U,* but they can be solved in sequential order beginning at the southwest corner of the grid:

$$L^{ij}_{SW} = \frac{A^{ij}_{SW}}{1 + \alpha U^{(i-1),(j-1)}_{SE}}$$

$$L^{ij}_W = A^{ij}_W + L^{ij}_{SW}U^{ij}_N - \alpha L^{ij}_{NW}U^{(i-1),(j+1)}_N$$

$$L^{ij}_{NW} = \frac{A^{ij}_S - L^{ij}_W U^{(i-1),j}_N}{1 + \alpha\left(U^{(i-1),(j+1)}_N + U^{(i-1),(j+1)}_{NE}\right)}$$

$$L^{ij}_S = \frac{A^{ij}_S - L^{ij}_{SW}U^{(i-1),(j-1)}_E - L^{ij}_W U^{(i-1),j}_{SE} - \alpha L^{ij}_{SW}U^{(i-1),(j-1)}_{SE}}{1 + \alpha U^{i,(j-1)}_{SE}}$$

$$\begin{aligned}L^{ij}_P &= A^{ij}_P - L^{ij}_{SW}U^{(i-1),(j-1)}_{NE} - L^{ij}_W U^{(i-1),j}_E - L^{ij}_{NW}U^{(i-1),(j+1)}_{SE} \\ &- L^{ij}_S U^{i,(j-1)}_N + 2\alpha\left(L^{ij}_{SW}U^{(i-1),(j-1)}_{SE} + L^{ij}_S U^{(i-1),(j+1)}_{SE}\right) \\ &+ 2\alpha L^{ij}_{NW}\left(U^{(i-1),(j+1)}_{NE} + U^{(i-1),(j+1)}_N\right)\end{aligned}$$

$$U^{ij}_N = \frac{A^{ij}_N - L^{ij}_W U^{(i-1),j}_{NE} - L^{ij}_{NW}U^{(i-1),(j+1)}_E - \alpha L^{ij}_{NW}U^{(i-1),(j+1)}_{NE}}{L^{ij}_P + \alpha L^{ij}_{NW}}$$

$$U^{ij}_{SE} = \frac{A^{ij}_{SE} - L^{ij}_S U^{i,(j-1)}_E}{L^{ij}_P + \alpha\left(L^{ij}_{SW} - L^{ij}_S\right)}$$

$$U^{ij}_E = \frac{A^{ij}_E - L^{ij}_S U^{i,(j-1)}_{NE} - \alpha L^{ij}_S U^{i,(j-1)}_{SE}}{L^{ij}_P}$$

$$U^{ij}_{SE} = \frac{A^{ij}_{NE}}{L^{ij}_P + \alpha L^{ij}_{NW}}$$

One considers that any matrix element that carries the index of a boundary node is zero.
The equation system using this approximation is solved by iteration. The updated residual is calculated

by the following equation:

$$LU\delta^{n+1} = \rho^n \tag{13}$$

The multiplication of the above equation by L^{-1} leads to:

$$\delta^{n+1} = L^{-1}\rho^n = R^n \tag{14}$$

where *R* is computed by:

$$R^{ij} = \frac{\rho^{ij} - L^{ij}_{SW}R^{(i-1),(j-1)} - L^{ij}_{S}R^{i,(j-1)}}{L^{ij}_{P}} - \frac{L^{ij}_{NW}R^{(i-1),(j+1)} - L^{ij}_{W}R^{(i-1),j}}{L^{ij}_{P}}. \tag{15}$$

When the computation of *R* is complete, we need to solve Eq. (14) using

$$\delta^{ij} = R^{ij} - U^{ij}_{N}\delta^{i,(j+1)} - U^{ij}_{NE}\delta^{(i+1),(j+1)} + U^{ij}_{E}\delta^{(i+1),j} + U^{ij}_{SE}\delta^{(i+1),(j-1)} \tag{16}$$

where the indexes *i,j* are decreasing.

3. Numerical experiments

In this section two problems are presented and solved using the above method. The first application is given by thermal evolution in circular cross section; the second is a solidification problem with complex geometry.

3.1 Simple geometry case

We start with the resolution of the thermal evolution of a slab with infinite length and circular cross section. The material has a unitary diffusivity, initially at the temperature of 0^oC, with Dirichlet boundary conditions (constant temperature equal to 1^oC). This problem is governed by the following expression (see [18]):

$$\frac{\partial\phi}{\partial t} = a\left(\frac{\partial^2\phi}{\partial\xi^2} + \frac{\partial^2\phi}{\partial\eta^2}\right), \tag{17}$$

where *a* is the thermal diffusivity. Applying the following boundary conditions:

$$\begin{aligned}&\phi(\xi,\eta,0) = 0;\\ &\phi(0,\eta,t) = \phi(1,\eta,t) = 1;\\ &\phi(\xi,0,t) = \phi(\xi,1,t) = 1,\end{aligned} \tag{18}$$

Eq. (17) has the following analytical solution in polar coordinates,

$$\Psi(r,t) = 1 - \sum_{n=1}^{+\infty}\frac{J_0(\mu_n r)}{J_1(\mu_n)}e^{-\mu_n^2 t}, \tag{19}$$

where μ_n is the squares of the equation $J_0(\mu) = 0$ and J_0 and J_1 are the Bessel functions of first degree, first and second order, respectively.

The use of curvilinear coordinates allows the use of a rectangular and time independent computational domain. In the FV method, one has to select the methods of approximating surfaces and volume integrals [13]. This is done using the grid shown in Fig. 3 generated by bilinear interpolation [19]. In order to avoid time step limitations, the time discretization was performed by the implicit Euler scheme. The time step used was $\Delta t = 1.0\times10^{-3}$ seconds.

This procedure was implemented in a FORTRAN code and the results are the following. Fig. 4 presents a comparison of the analytical solution, Eq. (19), and the numerical solution of Eq. (17).

A good agreement between numerical and analytical solutions is obtained, being the maximum error of 8% verified for 0.1seconds.

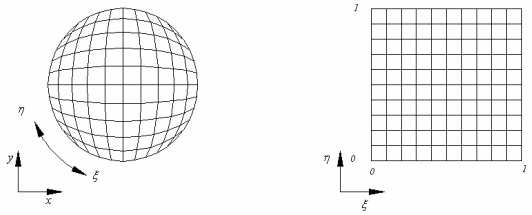

(a) (b)

Fig. 3. Used grid to solve the two dimensional heat conduction problem in irregular domain: (a) Physical domain; (b) Computational domain.

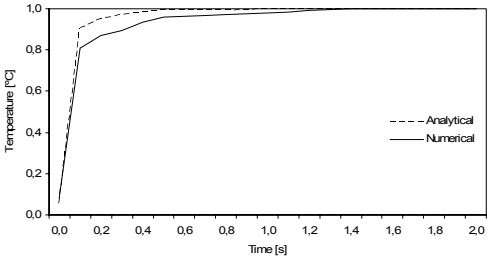

Fig. 4. Temperature versus time for the numerical and analytical solutions.

As was already mentioned, in these simulations three iterative solvers were used. The performance of each one is presented in Table 1 where is also made the comparison of the number of iterations to convergence using two distinct stopping criteria (10^{-3} and 10^{-5}). In our simulations the number of iterations was limited to one thousand.

The solution is convergent for the three used methods. Using a stopping criterion of 10^{-3} all the tested solvers show a good performance, with a slight advantage for the SIP method.

Increasing the precision for 10^{-5}, only the SIP method, presented in this work for the case of a computational cell of nine points, shows a good performance in terms of number of iterations, see Table 1.

To evaluate the difference in the value of the dependent variable (temperature) obtained by the SIP method using distinct stopping criteria (10^{-3} and 10^{-5}) the temperature difference is presented in Fig. 5. The maximum of temperature difference is about 10^{-7} ºC. Therefore, it seems that there is no reason to use the stopping criterion 10^{-5}.

3.2 Complex geometry case

The heat transfer problem arising from the study of the continuous metal casting process can be written by the following energy conservative equation:

$$\frac{\partial}{\partial t}\left(\rho C_P \phi\right) = \nabla \cdot \left(k \nabla \phi\right) + \dot{q}, \tag{20}$$

Tabel 1. Iterative methods performance.

Solver	Stop criteria 10^{-3}		Stop criteria 10^{-5}	
	Iter.	Residual	Iter.	Residual
Jacobi	8	2.56×10^{-4}	1000	2.03×10^{-5}
Gauss-Seidel	5	1.74×10^{-4}	1000	2.03×10^{-5}
SIP	2	9.55×10^{-4}	3	1.92×10^{-6}

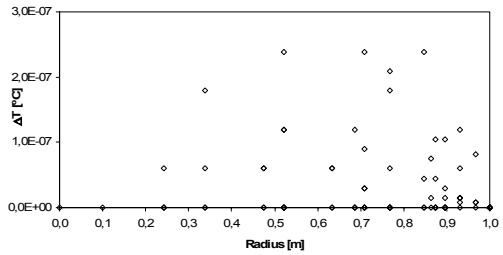

Fig. 5. Temperature difference using two distinct stopping criteria.

where the left hand side represents the transient contribution to the conservative energy equation (ϕ is the temperature); $\nabla \cdot \left(k \nabla \phi\right)$ is the diffusive contribution to the energy equation, k is the thermal conductivity and $\dot{q}$ represents the energy released during the phase change.

One also considers the physical properties ρ, C_P and k as constants analogously as done in [9, 20, 21].

The term $\dot{q}$ can be expressed as a function of effective solid material fraction f_s, part density ρ and enthalpy variation during the phase change Δh_f, by the following expression [20]:

$$\dot{q} = \frac{\partial}{\partial t}\left(\rho \Delta h_f f_s\right) \tag{21}$$

One can also decompose f_s in the following way:

$$\frac{\partial f_s}{\partial t} = \frac{\partial f_s}{\partial \phi}\frac{\partial \phi}{\partial t} \tag{22}$$

Assuming that Δh_f is independent of temperature and the material is isotropic, one substitutes Eqs. (21) and (22) in Eq. (20) and obtains

$$\frac{\partial \phi}{\partial t}\left(1 - \frac{\Delta h_f}{C_P}\frac{\partial f_s}{\partial \phi}\right) = \alpha\left(\nabla^2 \phi\right). \tag{23}$$

One uses the curvilinear coordinates, which transforms the domain into rectangular and time independent. The calculation is given by a uniform mesh of squares in *2D* (see Fig. 1), by the following transformation: $x_i = x_i\left(\xi_1, \xi_2\right)$ for *i=1,2* characterized by the Jacobian *J*:

$$J = \det\left[\frac{\partial x_i}{\partial \xi_j}\right]_{i,j}. \tag{24}$$

Therefore

$$\frac{\partial \phi}{\partial x_i} = \frac{\partial \phi}{\partial \xi_j}\frac{\partial \xi_j}{\partial x_i} = \frac{\partial \phi}{\partial \xi_j}\frac{\beta^{ij}}{J}, \tag{25}$$

where $\beta^{ij} = (-1)^{i+j}\det\left(J_{ij}\right)$ represents the cofactor in the Jacobian *J*.

Substituting Eq. (25) in Eq. (23) one obtains

$$J\frac{\partial \phi}{\partial t}\left(1 - \frac{\Delta h_f}{C_P}\frac{\partial f_s}{\partial \phi}\right) = \alpha\frac{\partial}{\partial \xi_j}\left(\frac{1}{J}\left(\frac{\partial \phi}{\partial \xi_m}B^{mj}\right)\right), \tag{26}$$

where the coefficient B^{mj} is defined by:

$$B^{mj} = \beta^{kj}\beta^{km} = \beta^{1j}\beta^{1m} + \beta^{2j}\beta^{2m}. \quad (27)$$

The coefficient B^{mj} becomes zero when the grid is orthogonal, therefore the use of these coefficients in the Eq. (26).

The second term of Eq. (26) can be expressed by

$$J\frac{\partial\phi}{\partial t}\left(1-\frac{\Delta h_f}{C_P}\frac{\partial f_s}{\partial\phi}\right) = C_1\frac{\partial\phi}{\partial\xi_1} + C_2\frac{\partial\phi}{\partial\xi_2} + C_{11}\frac{\partial^2\phi}{\partial\xi_1^2} + C_{12}\frac{\partial^2\phi}{\partial\xi_1\partial\xi_2} + C_{22}\frac{\partial^2\phi}{\partial\xi_2^2}, \quad (28)$$

where

$$C_1 = \frac{\partial J^{-1}}{\partial\xi_1}B^{11} + \frac{\partial J^{-1}}{\partial\xi_2}B^{12} + J^{-1}\left(\frac{\partial B^{11}}{\partial\xi_1} + \frac{\partial B^{12}}{\partial\xi_2}\right),$$

$$C_2 = \frac{\partial J^{-1}}{\partial\xi_1}B^{21} + \frac{\partial J^{-1}}{\partial\xi_2}B^{22} + J^{-1}\left(\frac{\partial B^{21}}{\partial\xi_1} + \frac{\partial B^{22}}{\partial\xi_2}\right),$$

$$C_{11} = J^{-1}B^{11},$$

$$C_{12} = J^{-1}\left(B^{21} + B^{12}\right),$$

$$C_{22} = J^{-1}B^{22}.$$

By the discretization, using the FV method, follows

$$\int_V \frac{\partial\phi}{\partial\xi_i}dV = \frac{\phi_E - \phi_W}{2}\Delta V$$

and the second order derivatives are approximated as follows:

$$\int_V \frac{\partial^2\phi}{\partial\xi_i^2}dV = \int_S \frac{\partial\phi}{\partial\xi_i}.\hat{n}.dS = \left(\frac{\partial\phi}{\partial\xi_i}\right)_e S_e - \left(\frac{\partial\phi}{\partial\xi_i}\right)_w S_w$$

$$\int_V \frac{\partial^2\phi}{\partial\xi_i\partial\xi_j}dV = \int_V \frac{\partial}{\partial\xi_i}\left(\frac{\partial\phi}{\partial\xi_j}\right)dV = = \frac{\left(\frac{\partial\phi}{\partial\xi_i}\right)_n S_n - \left(\frac{\partial\phi}{\partial\xi_i}\right)_s S_s}{\Delta\xi_{ic}}$$

The algebraic equation for a particular control volume in a two-dimensional domain, see Fig. 1, using curvilinear coordinates, can be established by:

$$Q_P = A_P\theta_P + A_E\theta_E + A_W\theta_W + A_N\theta_N + A_S\theta_S + A_{NE}\theta_{NE} + A_{SE}\theta_{SE} + A_{NW}\theta_{NW} + A_{SW}\theta_{SW}, \quad (29)$$

where

$$A_W = -\frac{C_1\Delta\xi_1\Delta\xi_2}{2} - \frac{C_{11}\Delta\xi_1\Delta\xi_2}{\Delta\xi_{1_c}}$$

$$A_E = -\frac{C_1\Delta\xi_1\Delta\xi_2}{\Delta\xi_{1_c}} - \frac{C_{11}\Delta\xi_1\Delta\xi_2}{\Delta\xi_{1_c}}$$

$$A_N = -\frac{C_2\Delta\xi_1\Delta\xi_2}{\Delta\xi_{2_c}} - \frac{C_{22}\Delta\xi_1\Delta\xi_2}{\Delta\xi_{2_c}}$$

$$A_S = \frac{C_2\Delta\xi_1\Delta\xi_2}{\Delta\xi_{2_c}} - \frac{C_{22}\Delta\xi_1\Delta\xi_2}{\Delta\xi_{2_c}}$$

$$A_{NW} = \frac{C_{12}\Delta\xi_1\Delta\xi_2}{4\Delta\xi_{1_c}\Delta\xi_{2_c}}$$

$$A_{SW} = A_{NE} = -A_{SE} = -A_{NW}$$

$$A_P = \left(1-\frac{\Delta h_f}{C_P}\frac{\partial f_s}{\partial\phi}\right)\frac{\Delta\xi_1\Delta\xi_2}{\Delta t}\frac{\rho C_P J}{k} - \left(A_W + A_E + A_N + A_S\right)$$

$$Q_P = \left(1-\frac{\Delta h_f}{C_P}\frac{\partial f_s}{\partial\phi}\right)\frac{\Delta\xi_1\Delta\xi_2}{\Delta t}\frac{\rho C_P J}{k}\phi^n$$

are valid for internal control volume. Different possibilities must be considered for heat transfer conditions on the boundary:

(i) Continuity condition for boundaries defined between continuous material [20]:

$$\left(\frac{\partial\phi}{\partial n}\right)_{m1} = \left(\frac{\partial\phi}{\partial n}\right)_{m2} \text{ and } \phi_{m1} = \phi_{m2}, \quad (30)$$

(ii) Newtonian heat transfer, for interfaces between metal and mold:

$$k_m\left(\frac{\partial\phi}{\partial n}\right)_m = h_i^*\left(\phi_m - \phi_s\right), \quad (31)$$

(iii) Convective heat transfer between mold and the environment:

$$k_m\left(\frac{\partial\phi}{\partial n}\right)_m = h_e\left(\phi_m - \phi_e\right), \quad (32)$$

where h_e and h^* are the convective heat transfer coefficients shown in the Table 2. The convective heat

transfer coefficients were determined by using the inverse heat conduction as described in [24]. The basic principle is to assume that the heat flux is a constant on a linear function of time within a given time interval. The whole description of this technique could be found in [25].

The complex geometry domain was divided into 17 polygons, Fig. 6, with 4 vertices (sub-domains) [22, 23].

In this case an analysis of heat transfer for casting process in two dimensions was made for the case during solidification. The idea was to determine the distribution of temperature and calculate the solidification time for the whole domain.

The definition of all coordinate lines in the interior of the domain is made by bilinear interpolation of the nodal position defined in the boundaries resulting in the grid showed in Fig. 7.

The physical characteristics of the material involved in the numerical simulation are shown in Table 3. In this case, the properties of the mold materials were considered as constant.

The environment temperature was considered to be 20ºC. To prevent the filling to be interrupted by premature solidification, the metal is cast into a hot mold.

Table 2. Convective heat transfer coefficients.

Interface	Convective heat transfer coefficients (W/m^{2}ºC)
Cast metal / mold	h_i=2500
Sub-domain 8/16	h_i=500
Sub-domain 11/17	h_i=500
Sub-domain 6/14	h_i=600
Mold / environment	h_e=150

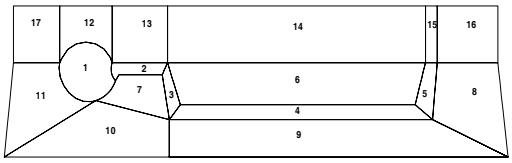

Fig. 6. Sub-domains of the complex geometry case.

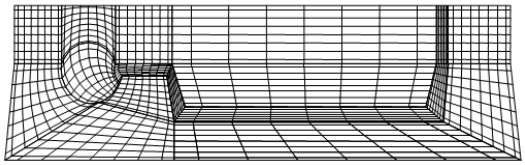

Fig. 7. Multi-block grid.

Therefore, the initial temperature field in the mold is considered uniform and equal to 300ºC. The initial temperature field in the part is also considered uniform, and equal to the liquidus temperature. The end of the phase change is determined by the solidus temperature.

Table 4 shows the performance of the three solvers under study for the seventeen blocks in which the complex geometry was divided (see Fig. 6). Since the analysis was made for each sub-domain, only some relevant sub-domains will be discussed further.

The sub-domain 1, which is the most complex geometrical structure, shows that after 1000 iterations the SIP method has better residual in comparison with the other two classical solvers. The same conclusion can be made for sub-domain 14 after 1000 iterations,

Table 3. Physical properties.

Property	Alloy AL 12Si	Grey cast-iron
Density (kg/m^3)	2670	7230
Conductivity (W/mºC)	185	38
Heat capacity (J/KgºC)	1260	750
Latent heat (KJ/Kg)	395	…
Liquidus temperature (ºC)	585	…
Solidus temperature (ºC)	575	…

Table 4. Iterative methods performance.

Block	Jacobi		Gauss-Seidel		SIP	
	Iter.	Res.	Iter.	Res.	Iter..	Res.
1	1000	1,51	1000	1,51	1000	$1{,}99\times10^{-3}$
2	1000	0,48	1000	0,46	2	$8{,}90\times10^{-4}$
3	1000	0,33	1000	0,33	1000	$1{,}05\times10^{-3}$
4	1000	2,28	1000	2,28	2	$8{,}64\times10^{-4}$
5	1000	0,52	1000	0,53	2	$9{,}18\times10^{-4}$
6	1000	3,32	1000	3,31	2	$1{,}66\times10^{-4}$
7	1000	0,59	1000	0,57	2	$1{,}54\times10^{-4}$
8	1000	1,65	1000	1,73	2	$4{,}57\times10^{-4}$
9	1000	1,78	1000	1,66	2	$6{,}41\times10^{-5}$
10	1000	1,66	1000	1,59	1000	$1{,}91\times10^{-3}$
11	1000	1,27	1000	1,15	2	$1{,}21\times10^{-4}$
12	1000	0,34	1000	0,34	3	$4{,}44\times10^{-5}$
13	1000	1,05	1000	0,90	2	$2{,}46\times10^{-4}$
14	1000	5,36	1000	5,47	1000	$6{,}19\times10^{-3}$
15	1000	0,25	1000	0,25	2	$2{,}85\times10^{-4}$
16	1000	0,77	1000	0,78	1000	$3{,}07\times10^{-3}$
17	1000	0,38	1000	0,37	1000	$1{,}31\times10^{-3}$

even though the higher simplicity of its geometry shows the worse residual result.

Sub-domain 7, which is a block with three boundaries in contact with the cast part, converges after only two iterations for SIP solver. For the other cited solvers no convergence has been shown after 1000 iterations.

Sub-domain 9, besides its similarity with sub-domain 14 in terms of geometry and boundary conditions, shows the best residual result for the SIP solver.

4. Conclusion

Adaptations of simple iterative methods (Jacobi and Gauss-Seidel) and the incomplete factorization method (strongly implicit procedure) to generalized curvilinear coordinates were presented and applied in simple and complex geometries through the multi-block grid technique.

Two test cases, a simple geometry (heat transfer in a circular cross-section) and a complex geometry (solidification case), are presented.

In the simple geometry case the performance of the adapted solvers herein expressed in terms of residual and number of iterations shows to have a very good performance with a slight advantage for the SIP solver. When the stopping criterion is changed from high precision to low precision residue, the corresponding temperature difference is insignificant. Therefore, the use of the latter stopping criterion does not have any significant change in the solution, having the advantage of reducing the computational time. For increasing the complexity of the geometry, the results showed that Jacobi and Gauss-Seidel solvers are not suitable. However, the SIP solver continues to have a reasonable performance. In conclusion, the strongly implicit procedure method, when combined with generalized curvilinear coordinates and multi-block grid technique, can be used in complex geometry problems when high precision results are not required.

Acknowledgment

This work has been supported by Centre for Research and Technology of Agro-Environment and Biological Sciences (CITAB).

R. De Almeida gratefully acknowledges the financial support from the R\&D unit *Matemática e Aplicções* (UIMA) of the University of Aveiro, sponsored through the Portuguese Foundation for Science and Technology (FCT) and co-financed by the European Community fund FEDER.

References

[1] D. J. Mavriplis, Unstructured Grid Techniques, *Annu. Rev. Fluid Mech.* 29(1997) 473-514.

[2] V. Feldheim and P. Lybaert, Solution of radial heat transfer problems with discrete transfer method applied to triangular meshes, *Journal of Computational and Applied Mathematics* 168 (2004) 179-190.

[3] F. C. Lockwood and N. G. Shah, A new radiation solution method for incorporation in general combustion prediction procedures, *18th International Symposium on Combustion, The Combustion Institute, Pittsburgh, PA* (1981) 1405-1414.

[4] B. Wiwatanapataphee, Y. H. Wu, J. Archapitak, P. F. Siew and B. Unyong, A numerical study of the turbulent flow of molten steel in a domain with a phase-change boundary, *Journal of Computational and Applied Mathematics.* 166 (2004) 307-319.

[5] G. Tryggvason, A. Esmaeeli and N. Al-Rawahi, Direct numerical simulations of flows with phase change, *Computers & Structures.* 83 (2005) 445-453.

[6] S. Dimova, M. Kaschiev, M. Koleva and D. Vasileva, Numerical analysis of radially nonsymmetric blow-up solutions of a nonlinear parabolic problem, *Journal of Computational and Applied Mathematics*. 97 (1998) 81-97.

[7] C. W. Lan and F. C. Chen, A finite volume method for solute segregation in directional solidification and comparison with a finite element method, *Comput. Methods Appl. Mech. Engrg.* 131 (1-2) (1996) 191-207.

[8] S. E. Shepel and S. Paolucci, Numerical simulation of filling and solidification of permanent mold casting, *Applied Thermal Engineering*. 22 (2002), 229-248.

[9] D. A. Knoll, W. B. Vanderheyden, V. A. Mousseau and D. B. Kothe, On preconditioning Newton-Krylov methods in solidifying flow application, *SIAM, J. Appl. Math.* 23(2) (2001) 381-397.

[10] M. Bellet and V. D. Fachinotti, ALE method for solidification modelling, *Comput. Methods. Appl. Mech. Engrg.* 193 (2004) 4355-4381.

[11] G. E. Schneider and M. Zedan, A modified Strongly Implicit procedure for the numerical solu-

tion of field problems, *Numer. Heat Transfer*. 4 (1) (1981) 1-19.

[12] M. Peric, Efficient semi-implicit solving algorithm for nine-diagonal coefficient matrix, *Numer. Heat Transfer*. 11(3) (1987) 251-279.

[13] J. H. Ferziger and M. Peric, *Computational Methods for Fluid Dynamics*, 2nd edition, Springer Verlag, Berlin, Heidelberg, New York USA, (1999).

[14] H. Pina, M*étodos Numéricos*, McGraw-Hill. (1995).

[15] J. C. Tannehill, D. A. Anderson and R. H. Pletcher, *Computational Fluid Mechanics and Heat Transfer*, 2nd edition, Taylor & Francis Ltd. (1997).

[16] S. E. Norris, *A Parallel Navier Stokes Solver for Natural convection and Free Surface Flow*. Ph.D Thesis, Faculty of Mechanical Engineering, University of Sydney, Australia, (2001).

[17] H. L. Stone, Iterative solution of implicit approximations of multidimensional partial differential equations, *SIAM, J. Numer. Anal.* 5 (1968) 530-558.

[18] H. S. Carslaw, J.C. Jaeger, *Conduction of Heat in Solids*. Clarendon Press, Oxford, (1959).

[19] J. F. Thompson, Z. U. A. Warsi and C. W. Mastin, *Numerical Grid Generation, Foundations and Applications*, Elsevier Science Publishing Co., Amsterdam, (1985).

[20] A. A. C. Monteiro. *Estudos do Comportamento Térmico de Moldações Metálicas para a Fundição Aplicando o Método das Diferenças Finitas Generalizadas* , Ph.D. Thesis, University of Minho, Braga, Portugal, (1996).

[21] N. Shamsundar and E. M. Sparrow, Analysis of multidimensional conduction phase change via the enthalpy model, *J. Heat Transfer*. 97 (1975) 333-340.

[22] E. Monteiro, A. A. C. Monteiro and A. Rouboa. Heat transfer simulation in the mould with generalize curvilinear formulation. *Journal of Pressure Vessel Technology*. 128 (2006) 462-466.

[23] E. Monteiro and A. Rouboa. Numerical simulation of the aluminium alloys solidification in complex geometries. *J. Mech. Sci. Tech.* 19(9) (2005) 1773-1780.

[24] A. Rouboa and E. Monteiro, Computational fluid dynamics analysis of greenhouse microclimates by heated underground tubes, *J. Mech. Sci. Tech.* 21 (12) (2007) 2196-2204.

[25] F. Lau, W. B. Lee, S. M. Xiong and B. C. Liu, A study of the interface heat transfer between an iron casting and a metallic mould, *J.Mat. Processing Technology*. 79 (1998) 25-29.

Professor Abel Rouboa obtained his P.h.D. (1994) in Fluid Dynamics at University of Paris VI and CEA, before joining the University of Evry Val d'E-ssonne, Paris, as assistant professor. In September 1999, he joined University of UTAD at Vila real, Portugal as assistant professor then in 2003 as associate professor. His teaching interests include heat transfer, fluid mechanics and numerical analysis. Professor Rouboa's research interests focus on Computational Fluid Dynamics emphasis on heat transfer. Currently, his research works is, strongly, linking with department of Mechanical Engineering and Applied Mechanics of University of Pennsylvania.